MONTE CARLO TRANSVERSE EMITTANCE STUDY ON Cs$_2$Te

F. Banfi[*], G. Ferrini[†], E. Pedersoli[†], S. Pagliara[†], C. Giannetti[†], G. Galimberti[†],
S. Lidia[‡], J. Corlett[‡], B. Ressel[§], F. Parmigiani[§,**].
[*] *DPMC, Université de Genève, Genève, Switzerland.*
[†] *Dipartimento di Matematica e Fisica, Università Cattolica, Brescia, Italy.*
[‡] *Lawrence Berkeley National Laboratory, Berkeley, CA USA.*
[§] *Sincrotrone Trieste, Basovizza-Trieste, Italy.*
[**] *Dipartimento di Fisica, Università di Trieste,Trieste, Italy.*

Abstract

The thermal emittance of photoelectrons in Cs$_2$Te thin films is investigated by a Monte Carlo simulation. The effects of electron-phonon scattering are discussed and the thermal emittance calculated for radiation wavelength at 265 nm and a spot radius of 1.5 mm. We find $\epsilon_{n,rms}$ = 0.56 mm-mrad. The dependence of $\epsilon_{n,rms}$ and the quantum yield on the electron affinity is also investigated. The data show the importance of considering the aging/contamination of the material to assess its emittance.

INTRODUCTION

High brightness electron beams are a fundamental tool to many applications ranging from electron microscopy to accelerator technology. In this context the transverse emittance of an electron beam at the surface of the photocathode is an important parameter. Semiconductor photocathodes are attractive because of their high quantum yield [1]. In particular, Cs$_2$Te is under investigation as a photoemitter for free electron lasers and advanced synchrotron radiation sources. Despite the fact that Cs$_2$Te has been studied extensively, most of the efforts have been devoted to issues such as the energy distribution of the photoemitted electrons, in conjunction with electron scattering, and thermal emittance of the photoejected electron beam under strong electric fields. The issues of the photoemitted electrons angular distribution and thermal emittance *at* the cathode have received comparatively little attention. In this work we investigate, via Monte Carlo (MC) simulations, the photoemitted electron distribution and transverse emittance at the surface of a Cs$_2$Te photocathode.

THE MODEL

The compound Cs$_2$Te is a p-type semiconductor with a band gap of 3.2 eV and an electron affinity that is roughly 0.3 eV. A schematic band diagram is illustrated in Fig. 1. Semiconductor materials are known to be good photoemitters because they are good absorbers and photoexcited electrons experience little electron-electron scattering. A large ratio between the band gap and the electron affinity is indicative of high quantum efficiencies for photons with energy greater than $E_g + E_A$ and less than $2E_g$ [2].
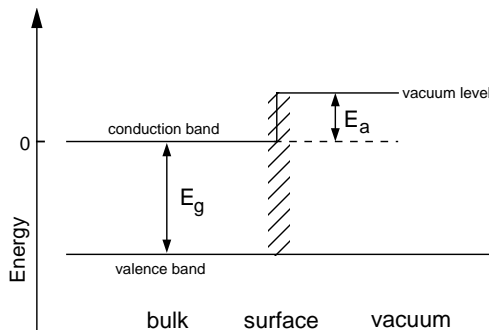
Figure 1: Energy band diagram for Cs$_2$Te. The energy gap separates the valence band (VB) from the conduction band (CB). The vacuum level is separated from the CB minimum by the electron affinity.

The MC simulation of photoemission from Cs$_2$Te follows a scheme first introduced to study electron scattering mechanism in metals [3] and successfully applied to simulate the quantum yield dependence on photon energy in Cs$_2$Te [4]. The calculations are based on the three step model for photoemission [5], which has proven to be a reliable model from which to interpret photoemission data in many materials, including Cs$_2$Te [6]. In the three step model a photoemitted electron is first photoexcited inside the material (step 1: photoexcitation), secondly it travels toward the sample surface (step 2: transport) and third it overcomes the surface barrier (step 3: emission).

We consider a 30 nm Cs$_2$Te polycrystalline layer deposited on a Mo substrate and use the microscopic parameters deduced from experimental data taken from [4]. We assume that every absorbed photon produces a photoexcited electron. The distributions of the electron kinetic energy within the material, E_{in}, momentum, p_{in}, and depth from the surface, z, are statistically determined at the beginning of the simulation as in reference [6] and are recalculated, after each scattering event, for every single photoexcited electron. The probability for an electron to travel a distance $z/\cos\theta_{in}$ in the forward direction, without scattering, is proportional to $\exp(-z/\lambda_p\cos\theta_{in})$, where λ_p is the electron mean free path, assumed to be energy-independent. With the Cs$_2$Te parameters and a photon energy $h\nu$=4.68 eV excited electrons are below the threshold for the onset

of electron-electron (e-e) scattering. Therefore, only quasi-elastic electron-phonon scattering is considered. Upon an electron-phonon scattering event, the electron energy is reduced by an amount E_p=5 meV [4] and the momentum direction is randomized over all solid angles. Since all solid angles are assumed equiprobable, the randomization process is then equivalent to all values of $\cos\theta_{in}$ being equiprobable, where θ_{in} is the polar angle for the electron trajectory inside the material. Only those photoexcited electrons that reach the surface with a kinetic energy ($E_{in,\perp}$) sufficient to overcome the surface potential barrier (the electron affinity, E_a) are photoemitted. This is schematically shown in Fig. 1. Electrons that reach the surface, but do not satisfy the above-mentioned condition, are reflected back into the semiconductor film. Electrons with $E_{in} < E_a$, or crossing the Cs_2Te/Mo interface, are eliminated from the simulation.

PHOTOEMITTED ELECTRON ANGULAR DISTRIBUTION

Electrons photoemitted from a cathode by photons well above threshold possess a spread in the transverse and longitudinal momentum components. The emittance of an electron bunch is a measure of its spread both in real and momentum space and depends on the spot size, the momentum distribution and the angular distribution. In order to estimate the emittance at the cathode surface, the photoemitted electron angular distribution is investigated.

Only electrons approaching the surface with sufficient energy will cross the semiconductor-vacuum interface. Given the total electron energy at the surface, E_{in}, an electron will be photoemitted only if the internal angle at the surface is lower than a critical angle θ_c: $\theta_{in} \leq \theta_c$, where $\theta_c \equiv \cos^{-1}\sqrt{E_a/E_{in}}$.

The relation between the internal and external polar angles is given by a solid-state analog of Snell's law due to conservation of transverse momentum at the interface:

$$\frac{\sin(\theta_{in})}{\sin(\theta_{out})} = \sqrt{\frac{E_{in} - E_a}{E_{in}}}. \tag{1}$$

where θ_{in} and θ_{out} are the polar angles for the electron trajectories inside and outside the sample surface respectively.

The calculated distribution of the photoemitted electrons is reported in Fig. 2. The calculation is performed following 10^5 electrons trajectories. The bin angular width is chosen equal to 0.36°. The distribution has a maximum for $\theta_{in} \sim 34°$ and all photoemitted electrons are found within an internal cone defined by an angle of value $max\{\theta_{in}\}$=63°. A physical model to explain this distribution must be considered. First, assuming a random distribution over polar angles, the probability of finding an electron in the range $[\theta_{in}, \theta_{in} + d\theta_{in}]$ is proportional to $\sin\theta_{in}d\theta_{in}$. Second, electrons with small θ_{in} have larger probability to reach the surface because of the shorter distance to travel in the forward direction (a distance proportional to $\exp(-z/\lambda_p\cos\theta_{in})$). Taking into account both
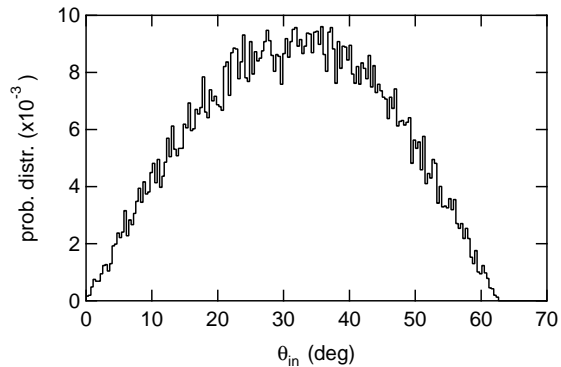
Figure 2: Angular probability distribution over internal angles θ_{in} of the electrons that are photoemitted.

of these mechanisms, integrating over z (the distance from the surface), and assuming that $\lambda_p \ll \alpha^{-1}$, where α is the absorption coefficient at 265 nm, the photoemitted electron distribution is proportional to $\sin(2\theta_{in})$ with $\theta_{in} < max\{\theta_c\}$. Hence, we expect a distribution peaked at θ_{in} =45° and with a sharp cut off at $max\{\theta_c\}$. As shown in Fig. 2, the calculated distribution can not be explained in terms of these two mechanisms alone. A third mechanism, due to the trajectory randomization upon scattering, needs to be considered.

The role of trajectory randomization

Electrons that reach the surface with energy E_{in} can equally contribute, because of momentum direction randomization due to scattering, to all θ_{in} within their critical cone, in the range $[0, \theta_c(E_{in})=a\cos\sqrt{E_a/E_{in}}]$. As the energy decreases, the critical cone decreases, privileging small values of θ_{in} in the distribution. Electrons of any energy can in fact contribute to emission about the forward direction, while only the most energetic ones can also contribute to emission at internal polar angles in proximity of $max\{\theta_{in}\}$. We simulate the emission process requiring that all photoemitted electrons have the same critical angle $max\{\theta_c\}$ regardless of their energy. In this case, the angular probability distribution over the internal angles θ_{in} of the photoemitted electrons is reported in Fig. 3. The distribution follows a curve proportional to $\sin(2\theta_{in})$ and has a sharp cutoff at $max\{\theta_c\}$, as expected. Moreover, changing E_a amounts to changing $max\{\theta_c\}$, with larger cut off angles associated to lower electron affinity values, as shown in Fig. 3.

The photoemitted electron angular distribution with respect to the external emission angle θ_{out} is reported in Fig. 4 and compared with the corresponding angular distribution over internal angles. The distribution over the external angles is smeared on the range $[0, 90°]$ and is peaked at lower polar angles as compared to what would be expected invoking the first two mechanisms alone.
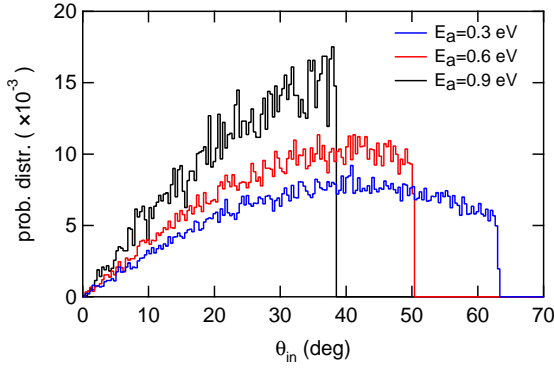
Figure 3: Angular probability distribution over internal angles θ_{in} of the electrons that are photoemitted.
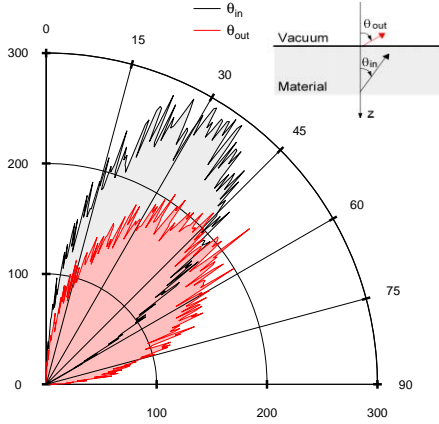
Figure 4: Electron count over internal angles (θ_{in}) (black histogram) and over external angles (θ_{out}) (red histogram) of the electrons that are photoemitted.
The inset shows the angle orientation.

The role of quasi-elastic scattering

We now investigate the role of electron energy loss, due to the quasi-elastic scattering , on the photoemitted electron angular probability distribution. To this purpose we simulate the angular probability distributions assuming both elastic, $E_p = 0$, and quasi-elastic scattering, $E_p = 5$meV. The distributions are equivalent, as can be seen in panel a) of Fig. 5. Each quasi-elastic scattering event reduces the electron energy by 5 meV and a photoemitted electron is found to scatter, on average, ~ 27 times, for an average photoemitted electron energy loss of ~ 130 meV. Therefore an important issue to be explained is the negligible effect on electrons angular distribution of a mean energy loss of about 9% of $max\{E_{in}\}$. The energy loss mainly affects the high energy part of the photoemitted electron's internal energy distribution. To understand the mechanism let us consider an electron with $E_{in}\sim E_a$. Upon scattering, this electron is eliminated from the distribution (electrons with $E_{in}<E_a$ cannot be photoemitted), but its energy position can be filled with an electron scattered from an higher energy position. This scattering-driven electron hopping to
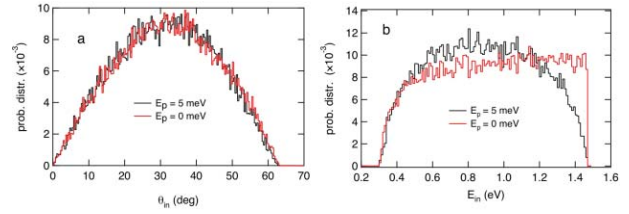
Figure 5: Panel a) Angular probability distribution over internal angles θ_{in} of the photoexcited electrons that are also photoemitted. Panel b) Energy probability distribution (10 meV bin) over internal kinetic energy E_{in} of the photoemitted electrons. E_{in} is the electron kinetic energy inside the sample. The histograms show the probability distributions calculated with the scattering event supposed elastic (red, E_p=0 eV) and quasi elastic (black, E_p=5 meV).

lower energies depopulates the high energy tail of the distribution (compare for instance the electron probability distribution for energies above 1.1 eV in the two histograms reported in Fig. 5 b) where no higher energy electrons are present to fill the vacancies.

The high energy tail of the probability distribution contributes equally to *all* emission angles and, for this reason, is the portion that least affects the photoemitted electron angular distribution. This can be appreciated noting that θ_c is monotonic with E_{in} and recalling the role of θ_c on the angular electron distribution. We thus conclude that the energy loss, due to the quasi-elastic electron-phonon (e-p) scattering, plays a negligible role in the photoemitted electron angular distribution. It is the trajectory randomization of e-p scattering that strongly affects the photoemitted electron angular distribution via the mechanism explained in the previous subsection.

TRANSVERSE EMITTANCE

The normalized transverse rms emittance is a measure of the electron beam phase space density. It may be deduced by measuring the rms beam divergence at the cathode for a given beam spot size. The normalized transverse rms emittance is defined as:

$$\epsilon_{n,rms} = \frac{1}{m_0 c}\sqrt{\sigma^2(x)\sigma^2(p_x) - \sigma^2(xp_x)} \qquad (2)$$

The correlation term $\sigma^2(xp_x)$ vanishes at the source, since the quantities x and p_x are uncorrelated, and $\overline{x}$ and $\overline{p_x}$ are null. Hence Eq. 2 reduces to:

$$\epsilon_{n,rms} = \frac{1}{m_0 c}p_{x,rms} \times x_{rms} \qquad (3)$$

The simulated normalized transverse momentum probability distribution *at* the cathode is reported in Fig. 6. The calculation is performed assuming a wavelength of 265 nm. From the distribution we obtain $p_{x,rms}/m_0c$=7.4×10^{-4}. We assume an hard edge laser spot size of radius
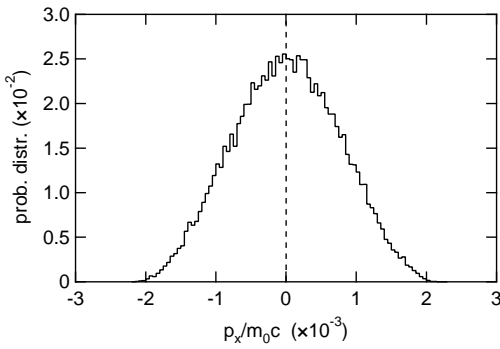
Figure 6: Probability distribution for the normalized transverse momentum at the cathode for photoemitted electrons. A bin of 5×10^{-5} is used for the normalized transverse momentum.
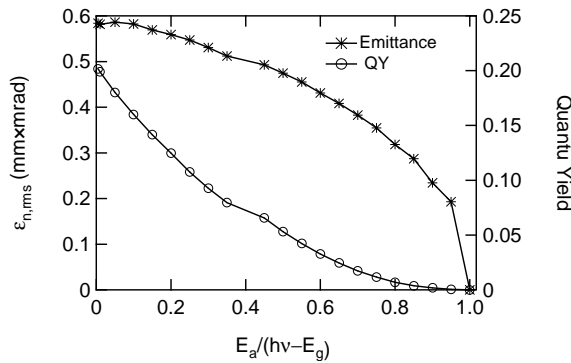
Figure 7: Quantum Yield (right axis) and normalized emittance at the cathode (left axis) as a function of electron affinity normalized to the maximum internal electron kinetic energy.

$r=1.5\times10^{-3}$. Making use of Eq. 3, we find $\epsilon_{n,rms}$ =0.56 mrad×mm.

Photocathode reliability is a key issue in the choice of material. Surface contamination, occurring during operation of the RF gun, affects the material electron affinity, which may affect $\epsilon_{n,rms}$ and the quantum yield. The results of the simulations are reported in Fig. 7. The graphs are plotted against a value of the electron affinity normalized with respect to the maximum electron kinetic energy. The clean sample corresponds, with the parameters in use, to a normalized electron affinity of 0.2, thus showing a QY of 12.5%, a value in good agreement with experimental data [7]. The graphs show that the main concern is the relatively rapid drop in QY as the electron affinity grows in excess of 0.3 eV. The decrease in the emittance is due to the preferential selection of electrons with forward directed momentum.

The results of the MC simulations are compared with those obtained by applying simple analytical calculations [8] in Fig. 8. The difference among the MC simulation and the analytical calculation is of significance for low value of $E_a/(h\nu - Eg)$, and amounts to almost 40% for E_a=0.3
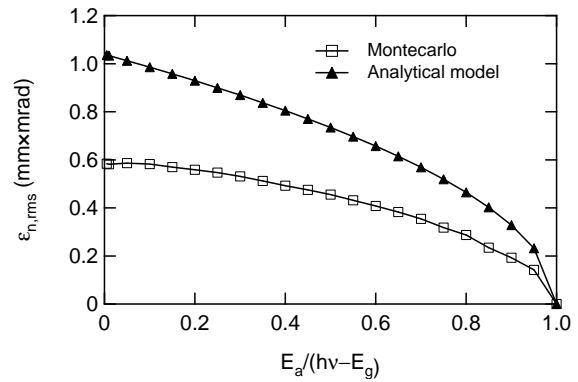
Figure 8: Normalized emittance at the cathode as a function of electron affinity normalized to the maximum electron kinetic energy.

eV ($E_a/(h\nu - Eg)$=0.2), i.e. for the value of E_a corresponding to clean Cs_2Te.

CONCLUSIONS

The photoemitted electron angular distribution and the transverse emittance at the cathode surface on Cs_2Te are investigated by Monte Carlo calculations. An explanation of the photoemitted electron angular distribution is given in terms of electron redistribution over all angles smaller than the proper critical angle for each electron. Electron-phonon scattering affects the photoemitted electron angular distribution through the randomization of momentum direction, whereas an average energy loss of $\sim$0.1 eV per photoemitted electron has a negligible effect. The transverse emittance, calculated for an impinging radiation at a wavelength of 265 nm, and a laser spot size of 1.5×10^{-3} m, is $\sim$ 0.56 mm-mrad. The effect of aging/contamination of the cathode on $\epsilon_{n,rms}$ and the QY is also investigated. Our results are an improvement of those obtained with analytical calculations, and underline the importance of statistical approaches to study photoemission processes where scattering is involved.

REFERENCES

[1] W. E. Spicer and A. Herrera-Gomez, SLAC-PUB-6306 (1993).

[2] A. H. Sommer, *Photoemissive materials*, New York, 1980.

[3] R. Stuart, et. al., Phys. Rev. **135**, A495 (1964).

[4] G. Ferrini, et. al., Solid State Comm. **106**, 21 (1998).

[5] W. E. Spicer, Phys. Rev. **112**, 114 (1958).

[6] R. A. Powell, et. al., Phys. Rev. B **8**, 3987 (1973).

[7] G. B. Fisher, et. al., Appl. Opt. **12**, 799 (1973).

[8] K. Flöttmann, TESLA-FEL 97-01 (1997).

[9] J. Clendenin and G. A. Mullhollan, SLAC-PUB-7760 (1998).